Lawrence Berkeley National Laboratory
Recent Work

Title
Search for Neutrinoless Double-β Decay in ^{76}Ge with the Majorana Demonstrator.

Permalink
https://escholarship.org/uc/item/0p03r70b

Journal
Physical review letters, 120(13)

Authors
Aalseth, CE
Abgrall, N
Aguayo, E
et al.

Peer reviewed

Search for Zero-Neutrino Double Beta Decay in ^{76}Ge with the MAJORANA DEMONSTRATOR

C.E. Aalseth,[1] N. Abgrall,[2] E. Aguayo,[1, a] S.I. Alvis,[3] M. Amman,[2] I.J. Arnquist,[1] F.T. Avignone III,[4, 5] H.O. Back,[6, 7, b] A.S. Barabash,[8] P.S. Barbeau,[9, c] C.J. Barton,[10] P.J. Barton,[2] F.E. Bertrand,[5] T. Bode,[11] B. Bos,[12] M. Boswell,[13, 14, 7] R.L. Brodzinski,[1, d] A.W. Bradley,[2, e] V. Brudanin,[15] M. Busch,[16, 7] M. Buuck,[3] A.S. Caldwell,[12] T.S. Caldwell,[14, 7] Y-D. Chan,[2] C.D. Christofferson,[12] P.-H. Chu,[13] J.I. Collar,[9] D.C. Combs,[6, 7] R.J. Cooper,[5, f] C. Cuesta,[3, g] J.A. Detwiler,[3, 2] P.J. Doe,[3] J.A. Dunmore,[3] Yu. Efremenko,[17] H. Ejiri,[18] S.R. Elliott,[13] J.E. Fast,[1] P. Finnerty,[14, 7, h] F.M. Fraenkle,[14, 7, i] Z. Fu,[3, j] B.K. Fujikawa,[2] E. Fuller,[1] A. Galindo-Uribarri,[5] V.M. Gehman,[13] T. Gilliss,[14, 7] G.K. Giovanetti,[19, 14, 7] J. Goett,[13] M.P. Green,[6, 7, 5, 14] J. Gruszko,[3, j] I.S. Guinn,[3] V.E. Guiseppe,[4, 10, 13] A.L. Hallin,[20] C.R. Haufe,[14, 7] L. Hehn,[2] R. Henning,[14, 7] E.W. Hoppe,[1] T.W. Hossbach,[1] M.A. Howe,[14, 7] B.R. Jasinski,[10] R.A. Johnson,[3] K.J. Keeter,[26] J.D. Kephart,[1] M.F. Kidd,[21, 13, 7] A. Knecht,[3, k] S.I. Konovalov,[8] R.T. Kouzes,[1] K.T. Lesko,[2, 22, 1] B.D. LaFerriere,[1] J. Leon,[3] L.E. Leviner,[6, 7] J.C. Loach,[23, 2] A.M. Lopez,[17] P.N. Luke,[2] J. MacMullin,[14, 7] S. MacMullin,[14, 7] M.G. Marino,[3, m] R.D. Martin,[24, 2] R. Massarczyk,[13] A.B. McDonald,[24] D.-M. Mei,[10, 13] S.J. Meijer,[14, 7] J.H. Merriman,[1] S. Mertens,[11, 25, 2] H.S. Miley,[1] M.L. Miller,[3] J. Myslik,[2] J.L. Orrell,[1] C. O'Shaughnessy,[14, 7, n] G. Othman,[14, 7] N.R. Overman,[1] W. Pettus,[3] D.G. Phillips II,[14, 7] A.W.P. Poon,[2] G. Perumpilly,[10] K. Pushkin,[10, o] D.C. Radford,[5] J. Rager,[14, 7] J.H. Reeves,[1, p] A.L. Reine,[14, 7] K. Rielage,[13] R.G.H. Robertson,[3] M.C. Ronquest,[13] N.W. Ruof,[3] A.G. Schubert,[3, q] B. Shanks,[5, 14, 7] M. Shirchenko,[15] K.J. Snavely,[14, 7] N. Snyder,[10] D. Steele,[13] A.M. Suriano,[12] D. Tedeschi,[4] W. Tornow,[16, 7] J.E. Trimble,[14, 7] R.L. Varner,[5] S. Vasilyev,[15, 17] K. Vetter,[2, r] K. Vorren,[14, 7] B.R. White,[13, 5] J.F. Wilkerson,[14, 7, 5] C. Wiseman,[4] W. Xu,[10, 13, 14, 7] E. Yakushev,[15] H. Yaver,[2] A.R. Young,[6, 7] C.-H. Yu,[5] V. Yumatov,[8] I. Zhitnikov,[15] B.X. Zhu,[13] and S. Zimmermann[2]

(MAJORANA Collaboration)

[1] *Pacific Northwest National Laboratory, Richland, WA 99354, USA*
[2] *Nuclear Science Division, Lawrence Berkeley National Laboratory, Berkeley, CA 94720, USA*
[3] *Center for Experimental Nuclear Physics and Astrophysics, and Department of Physics, University of Washington, Seattle, WA 98195, USA*
[4] *Department of Physics and Astronomy, University of South Carolina, Columbia, SC 29208, USA*
[5] *Oak Ridge National Laboratory, Oak Ridge, TN 37830, USA*
[6] *Department of Physics, North Carolina State University, Raleigh, NC 27695, USA*
[7] *Triangle Universities Nuclear Laboratory, Durham, NC 27708, USA*
[8] *National Research Center "Kurchatov Institute" Institute for Theoretical and Experimental Physics, Moscow, 117218 Russia*
[9] *Department of Physics, University of Chicago, Chicago, IL 60637, USA*
[10] *Department of Physics, University of South Dakota, Vermillion, SD 57069, USA*
[11] *Max-Planck-Institut für Physik, München, 80805 Germany*
[12] *South Dakota School of Mines and Technology, Rapid City, SD 57701, USA*
[13] *Los Alamos National Laboratory, Los Alamos, NM 87545, USA*
[14] *Department of Physics and Astronomy, University of North Carolina, Chapel Hill, NC 27514, USA*
[15] *Joint Institute for Nuclear Research, Dubna, 141980 Russia*
[16] *Department of Physics, Duke University, Durham, NC 27708, USA*
[17] *Department of Physics and Astronomy, University of Tennessee, Knoxville, TN 37916, USA*
[18] *Research Center for Nuclear Physics, Osaka University, Ibaraki, Osaka 567-0047, Japan*
[19] *Department of Physics, Princeton University, Princeton, NJ 08544, USA*
[20] *Centre for Particle Physics, University of Alberta, Edmonton, AB T6G 2E1, Canada*
[21] *Tennessee Tech University, Cookeville, TN 38505, USA*
[22] *Department of Physics, University of California, Berkeley, CA 94720, USA*
[23] *Shanghai Jiao Tong University, Shanghai, China*
[24] *Department of Physics, Engineering Physics and Astronomy, Queen's University, Kingston, ON K7L 3N6, Canada*
[25] *Physik Department and Excellence Cluster Universe, Technische Universität, München, 85748 Germany*
[26] *Department of Physics, Black Hills State University, Spearfish, SD 57799, USA*
[27] *Department of Nuclear Engineering, University of California, Berkeley, CA 94720, USA*

The MAJORANA Collaboration is operating an array of high purity Ge detectors to search for neutrinoless double-beta decay in ^{76}Ge. The MAJORANA DEMONSTRATOR comprises 44.1 kg of Ge detectors (29.7 kg enriched in ^{76}Ge) split between two modules contained in a low background shield at the Sanford Underground Research Facility in Lead, South Dakota. Here we present results from data taken during construction, commissioning, and the start of full operations. We achieve unprecedented energy resolution of 2.5 keV FWHM at $Q_{\beta\beta}$ and a very low background with no

observed candidate events in 10 kg yr of enriched Ge exposure, resulting in a lower limit on the half-life of 1.9×10^{25} yr (90% CL). This result constrains the effective Majorana neutrino mass to below 240 to 520 meV, depending on the matrix elements used. In our experimental configuration with the lowest background, the background is $4.0^{+3.1}_{-2.5}$ counts/(FWHM t yr).

Searches for neutrinoless double-beta ($\beta\beta(0\nu)$) decay test the Majorana nature of the neutrino [1]. The observation of this process would imply that total lepton number is violated and that neutrinos are Majorana particles [2]. A measurement of the $\beta\beta(0\nu)$ decay rate may also yield information on the absolute neutrino mass. Measurements of atmospheric, solar, and reactor neutrino oscillation [3] indicate a large parameter space for the discovery of $\beta\beta(0\nu)$ decay. Moreover, evidence from the SNO experiment [4] of a clear departure from non-maximal mixing in solar neutrino oscillation implies a minimum $\langle m_{\beta\beta} \rangle$ of ~15 meV for the inverted mass ordering scenario. This target is within reach of next-generation $\beta\beta(0\nu)$ searches. An experiment capable of observing this minimum rate would therefore help elucidate the Majorana or Dirac nature of the neutrino for inverted-ordering neutrino masses. Even if the ordering is normal, these experiments will have very high discovery probability [5]; a null result would improve the existing sensitivity by ~1 order of magnitude. A nearly background-free tonne-scale ^{76}Ge experiment would be sensitive to effective Majorana neutrino masses below ~15 meV. For recent comprehensive experimental and theoretical reviews on $\beta\beta(0\nu)$, see Refs. [6–14].

The MAJORANA DEMONSTRATOR is an array of isotopically enriched and natural Ge detectors searching for the decay of isotope ^{76}Ge. A primary technical goal of the experiment is the development and use of ultra-low activity materials and methods to suppress backgrounds to a low enough level to motivate the construction of a tonne-scale experiment. Here we present first results on the achieved background level and the corresponding $\beta\beta(0\nu)$ limit from an analysis of an initial detector exposure of 9.95 kg yr.

The DEMONSTRATOR utilizes the well-known benefits of enriched high-purity germanium (HPGe) detectors, including intrinsically low-background source material, understood enrichment process, excellent energy resolution, and sophisticated event reconstruction. We have assembled two modular HPGE arrays fabricated from ultra-pure electroformed copper. The enriched detectors are P-type, point-contact (P-PC) HPGe detectors [15–17]. These detectors allow a low-energy threshold permitting a variety of physics studies [18].

Each of the DEMONSTRATOR detectors has a mass of 0.6-1.1 kg. The two cryostats contain 35 detectors with a total mass of 29.7 kg fabricated with Ge material enriched to 88.1±0.7% in ^{76}Ge as measured by ICP-MS, and 23 detectors with a total mass of 14.4 kg fabricated from natural Ge (7.8% ^{76}Ge). The 69.8% yield of converting initial enriched material into Ge diodes is the highest achieved to date [19]. Module 1(2) houses 16.8 kg (12.9 kg) of enriched germanium detectors and 5.6 kg (8.8 kg) of natural germanium detectors. The two modules were installed sequentially with data collected from Module 1 (M1) while Module 2 (M2) was assembled.

A detailed description of the experimental setup can be found in Ref. [20] and some initial results were reported in Ref. [21]. Starting from the innermost cavity, two cryostat modules are surrounded by an inner layer of electroformed copper, an outer layer of commercially obtained C10100 copper, high-purity lead, an active muon veto [22], borated polyethylene, and polyethylene. The cryostats, copper, and lead shielding are all enclosed in a radon exclusion box that is purged with liquid-nitrogen boil-off gas. The experiment is located in a clean room at the 4850-foot level (1478 m, 4300 m.w.e.) of the Sanford Underground Research Facility (SURF) in Lead, South Dakota [23]. The radioassay program developed to ensure the apparatus met background goals is described in Ref. [24]. A parts-tracking database used to monitor exposures and inventory control is described in Ref. [25]. High voltage testing of components is described in Ref. [26] and the low-background readout electronics are described in Ref. [27, 28].

The data presented here are subdivided into six data sets, referred to as DS0 through DS5, distinguished by a significant experimental configuration changes. DS0 was a set of commissioning runs and was terminated to install the inner 2-inch electroformed copper shield and additional shielding. As a result, DS1 showed significantly reduced background. DS1 was terminated in order to test multisampling of the digitized waveforms, providing extended signal capture following an event for improved alpha background rejection. DS2 was terminated for the installation of Module 2. DS3 and DS4 consist of data taken from Module 1 and Module 2, respectively, with separate DAQ systems. DS5 consists of data taken after the DAQ systems were merged. The final installations of poly shielding enclosing the apparatus extended into DS5. We thus subdivided DS5 into two sub-ranges, DS5a and DS5b, where the latter corresponds to data taken after the detector was fully enclosed within the initial layer of poly shielding, allowing the establishment of a robust grounding scheme that reduced the electronic noise. The noise in DS5a impacted the pulse shape analysis, resulting in degraded background rejection. These changes define the difference between the data sets, with the com-

bination of DS1-4 and 5b having the lowest background (see the lower panel in Fig. 1).

The detector is calibrated using periodic (∼weekly) [228]Th line source calibration runs [29]. Event energies are reconstructed from the pulse amplitudes, using a trapezoidal filter algorithm whose parameters are tuned to minimize calibration source gamma line widths. We correct for (hole) charge trapping using the measured charge drift times, which greatly improves the resolution. The parameters of the peak shape are fit as a function of energy, which at the $\beta\beta(0\nu)$ Q value ($Q_{\beta\beta}$) yields a mixture ($\gtrsim$4:1) of a Gaussian (σ ∼1 keV) plus exGaussian (same σ, τ ∼2 keV), where the parameters are determined individually for each data set. This peak shape yields an average FWHM at $Q_{\beta\beta}$ of 2.52±0.08 keV (excluding DS5a), the best achieved to-date for a neutrinoless double-beta decay search. The uncertainty accounts for time variation, residual ADC non-linearities, and statistical uncertainties. Including DS5a, the average resolution is 2.66±0.08 keV.

Table I summarizes the key features of each data set. During each set, some detectors were inoperable. Furthermore, the system was not always collecting physics data due to calibration, systematic checks and construction activities. The live time and the active mass numbers within the table reflect these conditions.

The active mass calculations take into account the detector dead layers, measured with collimated [133]Ba source scans, as well as the detailed shape of each detector measured with an optical scanner. The active mass is ∼90% of the total mass with a systematic uncertainty of ∼1.4%, which dominates the uncertainty in the exposure. The exposure calculation, performed detector-by-detector, accounts for periods in which detectors are temporarily removed from the analysis due to instabilities. The exposure includes corrections for dead-time due to a 15-min cut to remove microphonic events coincident with liquid nitrogen fills and a 1-s period following muons detected in the veto system [30]. It also includes small losses due to the time for the digitizers to re-trigger after an event and cuts to remove pulser events, which are used to estimate dead time losses, gain shifts, and other instabilities. These cuts reduce the total live time by 1-5% depending on data set. The uncertainty in the live time is <0.5%. The results presented here are based on our open data. The blinded fraction of our data, set by a data parsing scheme, will be presented in future publications.

Data from the DEMONSTRATOR are first filtered by data cleaning routines to remove non-physical waveforms while retaining >99.9% of true physics events (ϵ_{DC}). Double-beta decay events are characterized as single-site events because the electron's deposit their energy over a small range (∼1 mm) compared to our ability to distinguish separate charge deposition sites as would arise from a typical multiple-Compton-scattered background

γ. We reject any events that trigger more than one detector within a 4-μs time window; the small associated signal inefficiency is negligible but we account for the associated dead time in our exposure calculation. Next we remove events whose waveforms are typical of multi-site energy deposits (ϵ_{AE}) while retaining 90%±3.5% of single-site events. This pulse shape discrimination [31] is based on the relationship between the maximum current and energy, similar to the cut described in Ref. [32], and is similarly tuned using [228]Th calibration source data. The efficiency uncertainty accounts for channel-, energy- and time-variation, as well as for the position distribution difference between calibration and $\beta\beta(0\nu)$ events, established using the MaGe simulation framework [33] built against Geant4 [34] and the detector signal simulation package, siggen [35].

The analysis also removes events that arise from external α particles impinging upon the passivated surface of our P-PC detectors. For such events, electron drift is negligible, and significant charge trapping of holes occurs in the immediate vicinity of the surface. The reconstructed energy of these events corresponds to the fraction of energy collected within the shaping time of our energy filter, resulting in energy degradation that sometimes populates the energy region near $Q_{\beta\beta}$. However, subsequent release of the trapped charge results in a significantly increased slope in the tail of the signal pulses. Quantification of this delayed charge recovery permits a highly effective reduction of this potential background using pulse shape discrimination [36] while retaining 99±0.5% (ϵ_{DCR}) of the bulk-detector events, as measured using [228]Th calibration source events. Collimated α-source measurements with a P-PC detector show that the waveform response and energy spectrum are a strong function of the distance from the point contact where the α impinges upon the passivated surface. The results indicate that the activity is most likely due to ^{210}Pb-supported [210]Po plated out as Rn daughters on the Teflon components of the detector mount.

True $\beta\beta(0\nu)$ events can exhibit energy degradation far from the $Q_{\beta\beta}$ due to their proximity to the crystal dead layer or due to the emission of bremsstrahlung resulting in energy deposition not fully contained within the active detector volume. Using the MaGe simulation framework, we estimate that 91±1% of true $\beta\beta(0\nu)$ events are fully contained (ϵ_{cont}). The uncertainty accounts for uncertainties in the detector geometry and the difference between simulation and literature values for bremsstrahlung rates and electron range.

All efficiencies are calculated individually for each data set with values listed in Table I. The product of the number of [76]Ge atoms (N), the live time (T), and the total signal efficiency (ϵ_{tot}) for each data set are also summarized in Table I.

Figure 1 shows the measured event spectrum above 100 keV using our event selection criteria. Background

TABLE I. A summary of the key parameters of each data set. The exposure calculation is done detector-by-detector. Symmetric uncertainties for the last digits are given in parentheses. The exposure numbers are for open data.

Data Set	Start Date	Hardware Distinction	Active Enr. Mass (kg)	Exposure (kg-yr)	ϵ_{AE}	ϵ_{DCR}	ϵ_{cont}	ϵ_{tot}	$NT\epsilon_{tot}\epsilon_{res}$ (10^{24}atoms y)
DS0	6/26/15	No Inner Cu Shield	10.69(16)	1.26(02)	$0.901^{+0.032}_{-0.035}$	$0.989^{+0.009}_{-0.002}$	0.908(11)	$0.808^{+0.031}_{-0.033}$	$6.34^{+0.25}_{-0.27}$
DS1	12/31/15	Inner Cu Shield added	11.90(17)	1.81(03)	$0.901^{+0.036}_{-0.040}$	$0.991^{+0.010}_{-0.005}$	0.909(11)	$0.811^{+0.035}_{-0.038}$	$9.23^{+0.41}_{-0.44}$
DS2	5/24/16	Multisampling	11.31(16)	0.29(01)	$0.903^{+0.035}_{-0.037}$	$0.986^{+0.011}_{-0.005}$	0.909(11)	$0.809^{+0.034}_{-0.035}$	$1.49^{+0.06}_{-0.07}$
DS3	8/25/16	M1 and M2 installed	12.63(19)	1.01(01)	$0.900^{+0.030}_{-0.031}$	$0.990^{+0.010}_{-0.003}$	0.909(11)	$0.809^{+0.030}_{-0.030}$	$5.18^{+0.20}_{-0.20}$
DS4	8/25/16	M1 and M2 installed	5.47(08)	0.28(00)	$0.900^{+0.031}_{-0.034}$	$0.992^{+0.011}_{-0.002}$	0.908(10)	$0.809^{+0.030}_{-0.032}$	$1.47^{+0.06}_{-0.06}$
DS5a	10/13/16	Integrated DAQ (noise)	17.48(25)	3.45(05)	$0.900^{+0.034}_{-0.035}$	$0.969^{+0.013}_{-0.013}$	0.909(13)	$0.792^{+0.034}_{-0.034}$	$17.17^{+0.76}_{-0.79}$
DS5b	1/27/17	Optimized Grounding	18.44(26)	1.85(03)	$0.900^{+0.031}_{-0.033}$	$0.985^{+0.014}_{-0.005}$	0.909(13)	$0.805^{+0.032}_{-0.032}$	$9.46^{+0.39}_{-0.39}$
Total				9.95(21)					$50.35^{+0.70}_{-0.73}$
Total (DS1-4,5b)				5.24(17)					$26.84^{+0.65}_{-0.68}$

projections based on our assay program and MaGe simulations predict a flat background between 1950 keV and 2350 keV after rejecting possible gamma peaks within that energy range. We exclude ±5 keV ranges (indicated in the figure by shading) centered at 2103 keV (^{208}Tl single escape peak), 2118 keV and 2204 keV (^{214}Bi). We also ignore events near $Q_{\beta\beta}$ between 2034 keV and 2044 keV. The backgrounds are summarized in Table II along with the corresponding continuum background index (BI) assuming a flat profile. Uncertainties are computed using Feldman-Cousins intervals [37]. All six data sets are nearly background free at the present exposure and therefore we use all for a $T^{0\nu}_{1/2}$ limit.

TABLE II. The background (BG) within the defined 360-keV window for each of the data sets. The background index (BI, column 3) is given in units of counts/(keV kg yr). The optimum ROI width for each data set is given in column 4 and the resulting expected background counts within that ROI is given in the final column. The final row provides a summary for the lowest expected background data partition.

Data Set	Window Counts	BI $\times 10^{-3}$	ROI (keV)	ROI BG (counts)
DS0	11	$24.3^{+8.4}_{-7.0}$	3.93	0.120
DS1	3	$4.6^{+3.5}_{-2.9}$	4.21	0.035
DS2	0	<12.3	4.34	0.000
DS3	0	<3.6	4.39	0.000
DS4	0	<12.7	4.25	0.000
DS5a	10	$8.0^{+3.1}_{-2.6}$	4.49	0.125
DS5b	0	<1.9	4.33	0.000
Total	24	$6.7^{+1.4}_{-1.4}$	4.32	0.288
DS1-4,5b	3	$1.6^{+1.2}_{-1.0}$		0.036

After all cuts in DS0-5, there are 24 events within the 360-keV background window. This results in a

background index for the summed spectrum of 17.8±3.6 counts/(FWHM t yr) or $(6.7\pm1.4)\times10^{-3}$ counts/(keV kg yr). In the context of background rates relevant for future data taking and for a next-generation $\beta\beta(0\nu)$ experiment, we compute the background from the lowest expected background configuration (DS1-4,5b), which corresponds to $4.0^{+3.1}_{-2.5}$ counts/(FWHM t yr) or $1.6^{+1.2}_{-1.0}$ counts/(keV kg yr). This background level is statistically consistent with GERDA's best-achieved background to date for a $\beta\beta(0\nu)$ search, $2.9^{+1.8}_{-1.2}$ counts/(FWHM t y) for a resolution of 2.9 keV [38].

The half-life limit can be approximated as a Poisson-process search in an optimized region-of-interest (ROI) surrounding the peak energy. The ROI is optimized based on the achieved background level similarly to Ref. [5] except that the measured peak-shape function was used in place of the Gaussian assumption[1]. The result varies for individually-considered data sets as given in Table II and the exposure-weighted-average optimal ROI is 4.32 keV, with corresponding additional efficiency $\epsilon_{res} = 0.899\pm0.005$. This resolution efficiency factor only applies for this counting-measurement analysis and not for the spectrum fits described later. The measured background index corresponds to 0.29 expected total background counts in the optimized ROI near $Q_{\beta\beta}$. The lower limit on the half-life is thus approximately given by:

$$T^{0\nu}_{1/2} > \frac{\ln(2)NT\epsilon_{tot}\epsilon_{res}}{S},\qquad(1)$$

where S is the upper limit on the number of signal events that can be attributed to $\beta\beta(0\nu)$. Using the Feldman-Cousins approach [37] for 0 observed counts with an expected background of 0.29 gives $S=2.15$ at 90% CL. This results in a ^{76}Ge $\beta\beta(0\nu)$ half-life limit of 1.6×10^{25} yr.
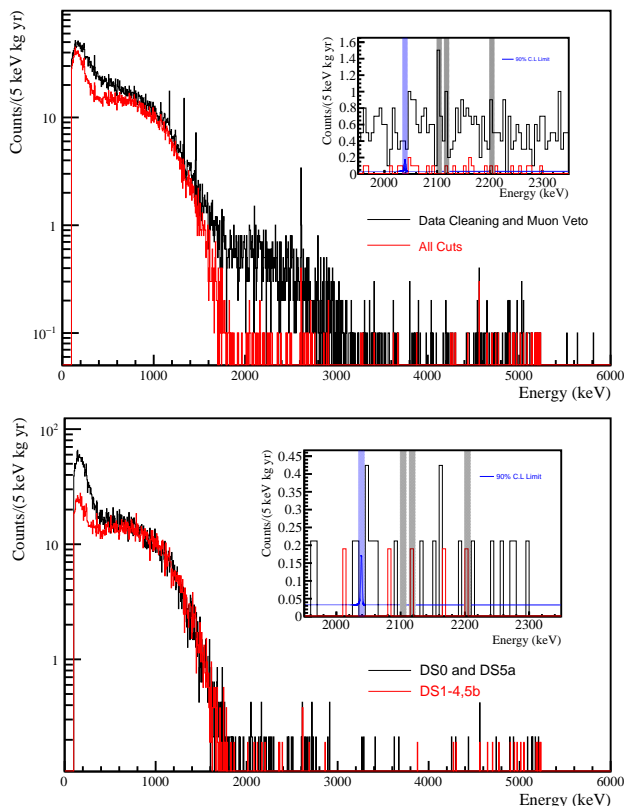
---

[1] See Eqn. B4 in Ref. [5].

10^{26} yr for a 100 kg yr exposure.

a Present address: Intel Corp., 2111 NE 25th Ave, Hilsboro, OR 97124, USA
b Present address: Pacific Northwest National Laboratory, Richland, WA 99354, USA
c Present address: Department of Physics, Duke University, Durham, NC 27708, USA, Triangle Universities Nuclear Laboratory, Durham, NC 27708, USA
d Deceased
e Present address: 775 Heinz Ave Berkeley, CA 94710, USA
f Present address: Nuclear Science Division, Lawrence Berkeley National Laboratory, Berkeley, CA 94720, USA
g Present address: Centro de Investigaciones Energticas, Medioambientales y Tecnolgicas, CIEMAT, 28040, Madrid, Spain
h Present address: Applied Research Associates, Inc., 8537 Six Forks Road, Raleigh, NC 27615, USA
i Present address: Institute for Nuclear Physics, Karlsruhe Institute of Technology, 76344 Eggenstein-Leopoldshafen, Germany
j Present address: Department of Physics, Massachusetts Institute of Technology, Cambridge, MA 02139, USA
k Present address: Paul Scherrer Institut, 5232 Villigen PSI, Switzerland
l Present address: Physics Division, Lawrence Berkeley National Laboratory
m Present address: tado GmbH, Sapporobogen 6-8, 80637 Munich, Germany
n Present address: Los Alamos National Laboratory, Los Alamos, NM 87545, USA
o Present address: Physics Department, University of Michigan, Ann Arbor, MI 48109, USA
p Present address: 216 Abert Avenue, Richland, WA 99352, USA
q Present address: OneBridge Solutions, Seattle, WA, USA
r Alternate address: Department of Nuclear Engineering, University of California, Berkeley, CA, USA

[1] Zralek M 1997 *ACTA Phys. Pol. B* **28** 2225
[2] Schechter J and Valle J W F 1982 *Phys. Rev. D* **25** 2951
[3] Patrignani C *et al.* 2016 *Chin. Phys. C* **40** 100001
[4] Ahmed S N *et al.* 2004 *Phys. Rev. Lett.* **92** 181301
[5] Agostini M, Benato G and Detwiler J 2017 *Phys. Rev. D* **96** 053001
[6] Avignone III F T, Elliott S R and Engel J 2008 *Rev. Mod. Phys.* **80** 481
[7] Barabash A S 2011 *Phys. Part. Nucl.* **42** 613
[8] Rodejohann W 2011 *Int. J. Mod. Phys. E* **20** 1833
[9] Elliott S R 2012 *Mod. Phys. Lett. A* **27** 1230009
[10] Vergados J D, Ejiri H and Šimkovic F 2012 *Rep. Prog. Phys.* **75** 106301
[11] Cremonesi O 2013 *Nucl. Phys. B Proc. Supp.* **237** 7 (*Preprint* arXiv:1212.4885)
[12] Schwingenheuer B 2013 *Ann. der Physik* **525** 269 (*Preprint* arXiv:1210.7432)
[13] Elliott S R and Franz M 2015 *Rev. Mod. Phys.* **87** 137
[14] Henning R 2016 *Rev. Phys.* **1** 29
[15] Luke P N, Goulding F S, Madden N W and Pehl R H 1989 *IEEE Trans. Nucl. Sci.* **36** 926
[16] Barbeau P S, Collar J I and Tench O 2007 *JCAP* **09** 009
[17] Aguayo E *et al.* 2011 sLAC eConf C110809 (*Preprint* arXiv:1109.6913)
[18] Abgrall N *et al.* 2017 *Phys. Rev. Lett.* **118** 161801
[19] Abgrall N *et al.* 2017 *Nucl. Instrum. Meth. A* **877** 314 (*Preprint* arXiv:1707.06255)
[20] Abgrall N *et al.* 2014 *Adv. High Energy Phys.* **2014** 365432
[21] Elliott S *et al.* 2017 *J. Phys.: Conf. Ser.* **888** 012035
[22] Bugg W, Efremenko Yu and Vasilyev S 2014 *Nucl. Instrum. Meth. A* **758** 91
[23] Heise J 2015 *J. Phys. Conf. Ser.* **606** 1
[24] Abgrall N *et al.* 2016 *Nucl. Instrum. Meth. A* **828** 22
[25] Abgrall N *et al.* 2015 *Nucl. Instrum. Meth. A* **779** 52
[26] Abgrall N *et al.* 2016 *Nucl. Instrum. Meth. A* **823** 83
[27] Barton P *et al.* 2011 *IEEE Nucl. Sci. Symp. Conf. Rec.* 1976 proceedings of 2011 IEEE Nucl. Sci. Symp. and Med. Imag. Conf. (NSS/MIC)
[28] Guinn I *et al.* 2015 *J. Phys. Conf. Ser.* **606** 012004
[29] Abgrall N *et al.* 2017 *Nucl. Instrum. Meth. A* **872** 16
[30] Abgrall N *et al.* 2017 *Astro. Phys.* **93** 70 (*Preprint* arXiv:1602.07742)
[31] Cuesta C and Majorana 2017 *J. Phys.: Conf. Ser.* **888** 012240
[32] Agostini M *et al.* 2013 *Eur. Phys. J. C* **73** 2583
[33] Boswell M *et al.* 2011 *IEEE Trans. Nucl. Sci.* **58** 1212
[34] Agostinelli S *et al.* 2003 *Nucl. Instrum. Meth. A* **506** 250

[35] Radford D C *et al.* to be published. siggen software available from the authors at svn URL `http://radware.phy.ornl.gov/MJ/mjd_siggen/`

[36] Gruszko J *et al.* 2017 *J. Phys.: Conf. Ser.* **888** 012079

[37] Feldman G J and Cousins R D 1998 *Phys. Rev. D* **57** 3873

[38] Agostini M *et al.* 2017 (*Preprint* arXiv:1710.07776)

[39] Verkerke W and Kirkby D 2003 The roofit toolkit for data modeling (*Preprint* arXiv:1203.1547)

[40] Schott G 2012 Roostats for searches (*Preprint* arXiv:1203.1547)

[41] Agostini M *et al.* 2017 *Nature* **544** 47 (*Preprint* 1703.00570)

[42] Read A L 2000 *CERN OPEN-2000-205* URL `http://cds.cern.ch/record/451614`

[43] Engel J and Menéndez J 2017 *Rep. Prog. Phys.* **80** 046301

[44] Menéndez J, Poves A, Caurier E and Nowacki F 2009 *Nucl. Phys. A* **818** 139

[45] Horoi M and Neacsu A 2016 *Phys. Rev. C* **93** 024308

[46] Barea J, Kotila J and Iachello F 2015 *Phys. Rev. C* **91** 034304

[47] Hyvärinen J and Suhonen J 2015 *Phys. Rev. C* **91** 024613

[48] Šimkovic F, Rodin V, Faessler A and Vogel P 2013 *Phys. Rev. C* **87** 045501

[49] Vaquero N L, rodríguez T R and Egido J L 2013 *Phys. Rev. Lett.* **111** 142501

[50] Yao J M *et al.* 2015 *Phys. Rev. C* **91** 024316

[51] Kotila J and Iachello F 2012 *Phys. Rev. C* **85** 034316

[52] Mirea M, Pahomi T and Stoica S 2015 *Rom. Rep. Phys.* **67** 872

[53] Gando A *et al.* 2016 *Phys. Rev. Lett.* **117** 082503

[54] Albert J B *et al.* 2017 (*Preprint* arXiv:1707.08707)

[55] Abgrall N *et al.* 2017 (*Preprint* arXiv:1709.01980)